Sex-specific silencing of X-linked genes by Xist RNA

Srimonta Gayen, Emily Maclary, Michael Hinten, and Sundeep Kalantry[1]

Department of Human Genetics, University of Michigan Medical School, Ann Arbor, MI 48109

Edited by David C. Page, Whitehead Institute, Cambridge, MA, and approved December 11, 2015 (received for review August 11, 2015)

X-inactive specific transcript (Xist) long noncoding RNA (lncRNA) is thought to catalyze silencing of X-linked genes *in cis* during X-chromosome inactivation, which equalizes X-linked gene dosage between male and female mammals. To test the impact of Xist RNA on X-linked gene silencing, we ectopically induced endogenous Xist by ablating the antisense repressor Tsix in mice. We find that ectopic Xist RNA induction and subsequent X-linked gene silencing is sex specific in embryos and in differentiating embryonic stem cells (ESCs) and epiblast stem cells (EpiSCs). A higher frequency of $X^{\Delta Tsix}Y$ male cells displayed ectopic Xist RNA coating compared with $X^{\Delta Tsix}X$ female cells. This increase reflected the inability of $X^{\Delta Tsix}Y$ cells to efficiently silence X-linked genes compared with $X^{\Delta Tsix}X$ cells, despite equivalent Xist RNA induction and coating. Silencing of genes on both Xs resulted in significantly reduced proliferation and increased cell death in $X^{\Delta Tsix}X$ female cells relative to $X^{\Delta Tsix}Y$ male cells. Thus, whereas Xist RNA can inactivate the X chromosome in females it may not do so in males. We further found comparable silencing in differentiating $X^{\Delta Tsix}Y$ and 39,$X^{\Delta Tsix}$ ($X^{\Delta Tsix}O$) ESCs, excluding the Y chromosome and instead implicating the X-chromosome dose as the source of the sex-specific differences. Because $X^{\Delta Tsix}X$ female embryonic epiblast cells and EpiSCs harbor an inactivated X chromosome prior to ectopic inactivation of the active $X^{\Delta Tsix}$ X chromosome, we propose that the increased expression of one or more X-inactivation escapees activates Xist and, separately, helps trigger X-linked gene silencing.

Xist | Tsix | X inactivation | embryonic stem cells | epiblast stem cells

X inactivation represents a paradigm of epigenetic regulation and long noncoding RNA (lncRNA) function. In *XX* female cells, one of the two X chromosomes undergoes transcriptional silencing (1). Moreover, replicated copies of the active and inactive X chromosomes faithfully maintain their respective transcriptional states through many cell division cycles (2–5).

X inactivation requires the X-inactive specific transcript (Xist) (6–8), a lncRNA that is selectively expressed from and physically coats the future inactive X chromosome (9–12). Xist RNA enables X-linked gene silencing by recruiting protein complexes to the inactive X (13–15). Female mouse embryos that inherit a paternal *Xist* mutation die due to defects in imprinted X inactivation of the paternal X chromosome in extraembryonic tissues (8, 16, 17). Xist is also required in the epiblast-derived embryonic cells, which undergo random X inactivation of either the maternal or the paternal X chromosome. Xist heterozygote fetal cells exhibit inactivation of only the X chromosome with an intact *Xist* locus, suggesting that *Xist* is necessary to choose the X chromosome to be inactivated (7, 18, 19). That the Xist-mutant X chromosome is not selected for inactivation, however, precludes assigning to Xist RNA a gene silencing role in the epiblast lineage.

Ectopic expression studies have, however, demonstrated that Xist RNA can silence genes, albeit in a context-dependent manner. Xist transgenes integrated into autosomes can silence neighboring autosomal sequences, but the effect is quite variable. Whereas multicopy *Xist* transgenes or transgenes driven by artificial promoters often display Xist RNA induction and coating of autosomes *in cis* accompanied by a degree of silencing of adjacent host sequences (20–28), large single-copy Xist genomic transgenes do not (19, 28, 29). The sequence composition and the chromatin context at the site of transgene integration as well as the level of Xist expression are confounding variables that may influence the ability of transgenic Xist RNA to silence.

We therefore sought to systematically test the impact of Xist RNA on gene silencing by ectopically inducing Xist from the endogenous locus, thus ensuring that the *cis*-regulatory elements necessary for robust Xist expression are intact. We previously generated male and female embryonic stem cells (ESCs) and epiblast stem cells (EpiSCs) that harbor an X chromosome with a null mutation in the Xist antisense repressor Tsix ($X^{\Delta Tsix}$) (30). A subset of differentiating $X^{\Delta Tsix}Y$ and $X^{\Delta Tsix}X$ cells display ectopic Xist RNA coating of the $X^{\Delta Tsix}$; thus, male cells harbor a single Xist RNA coat and females possess two Xist coats. These populations enabled us to assess the ability of Xist RNA to silence X-linked genes in males and in females.

Unexpectedly, we observed sex-specific differences in the frequency of cells that induced Xist from the active $X^{\Delta Tsix}$ and silenced X-linked genes once Xist was ectopically induced, both in vitro and in vivo. We found that a higher percentage of $X^{\Delta Tsix}Y$ cells displayed ectopic Xist RNA coating compared with $X^{\Delta Tsix}X$ cells. This increase reflected the inability of $X^{\Delta Tsix}Y$ cells to efficiently silence X-linked genes upon ectopic Xist induction compared with $X^{\Delta Tsix}X$ cells, despite equivalent levels of Xist expression and RNA coating. We discuss possible underlying reasons for these differences, including the requirement of two X chromosomes to physically interact, epigenetic variation on the $X^{\Delta Tsix}$ between the sexes, and differences in developmental timing between male and female embryos. The comparative analysis compels us to propose that the higher X-chromosomal dose in females, potentially acting through gene(s) that escape X inactivation, induces Xist and, separately, silences X-linked genes once Xist is induced. The increased dosage of such a factor(s) in females compared with males may explain why females undergo X inactivation and males do not.

Results

ESCs Display a Sex-Specific Difference in the Frequency of Ectopic Xist RNA Coating. To ectopically induce Xist, we differentiated multiple control wild-type (WT) *XY* and *XX* and mutant $X^{\Delta Tsix}Y$ and $X^{\Delta Tsix}X$ ESC lines (see *SI Appendix*, Fig. S1 for map of the ΔTsix

Significance

In mammals, the inequality posed by the difference in the number of X chromosomes between *XX* females and *XY* males is remedied by silencing genes along one of the two X chromosomes in females. This process, termed X-chromosome inactivation, is believed to be triggered by X-inactive specific transcript (Xist) RNA. Here we find that Xist RNA can silence X-linked genes efficiently in females but not in males. Thus, Xist RNA is insufficient to inactivate the X chromosome. Our results further suggest that both Xist induction and X-linked gene silencing are orchestrated by the handful of genes that do not undergo X inactivation in females. The increased dosage of one or more such factors in females vs. males may explain why females undergo X inactivation and males do not.

Author contributions: S.G., E.M., and S.K. designed research; S.G. and E.M. performed research; M.H. contributed new reagents/analytic tools; S.G., E.M., and S.K. analyzed data; and S.G., E.M., and S.K. wrote the paper.

The authors declare no conflict of interest.

This article is a PNAS Direct Submission.

[1]To whom correspondence should be addressed. Email: kalantry@umich.edu.

This article contains supporting information online at www.pnas.org/lookup/suppl/doi:10.1073/pnas.1515971113/-/DCSupplemental.

mutant allele) (30, 31). We assessed ectopic Xist RNA coating every 2 d over a period of 10 d by RNA fluorescence in situ hybridization (FISH). WT male *XY* ESC lines did not display Xist RNA-coated nuclei during differentiation. However, mutant male $X^{\Delta Tsix}Y$ lines exhibited three classes of nuclei: some had strong Xist RNA coating, resembling Xist RNA coating in female cells, some had weak Xist RNA coating, and some lacked Xist RNA coating altogether. Strong Xist RNA-decorated $X^{\Delta Tsix}Y$ nuclei reached a maximum of between 40% and 58% of all nuclei at day 6 (d6) of differentiation, before decreasing to ∼30% at d10 (Fig. 1*A*). Weak Xist RNA-coated $X^{\Delta Tsix}Y$ nuclei peaked at 18–22% at d4 and decreased to ∼8% at d10 of differentiation.

Undifferentiated female WT *XX* and mutant $X^{\Delta Tsix}X$ ESCs harbor two active X chromosomes, which are randomly inactivated

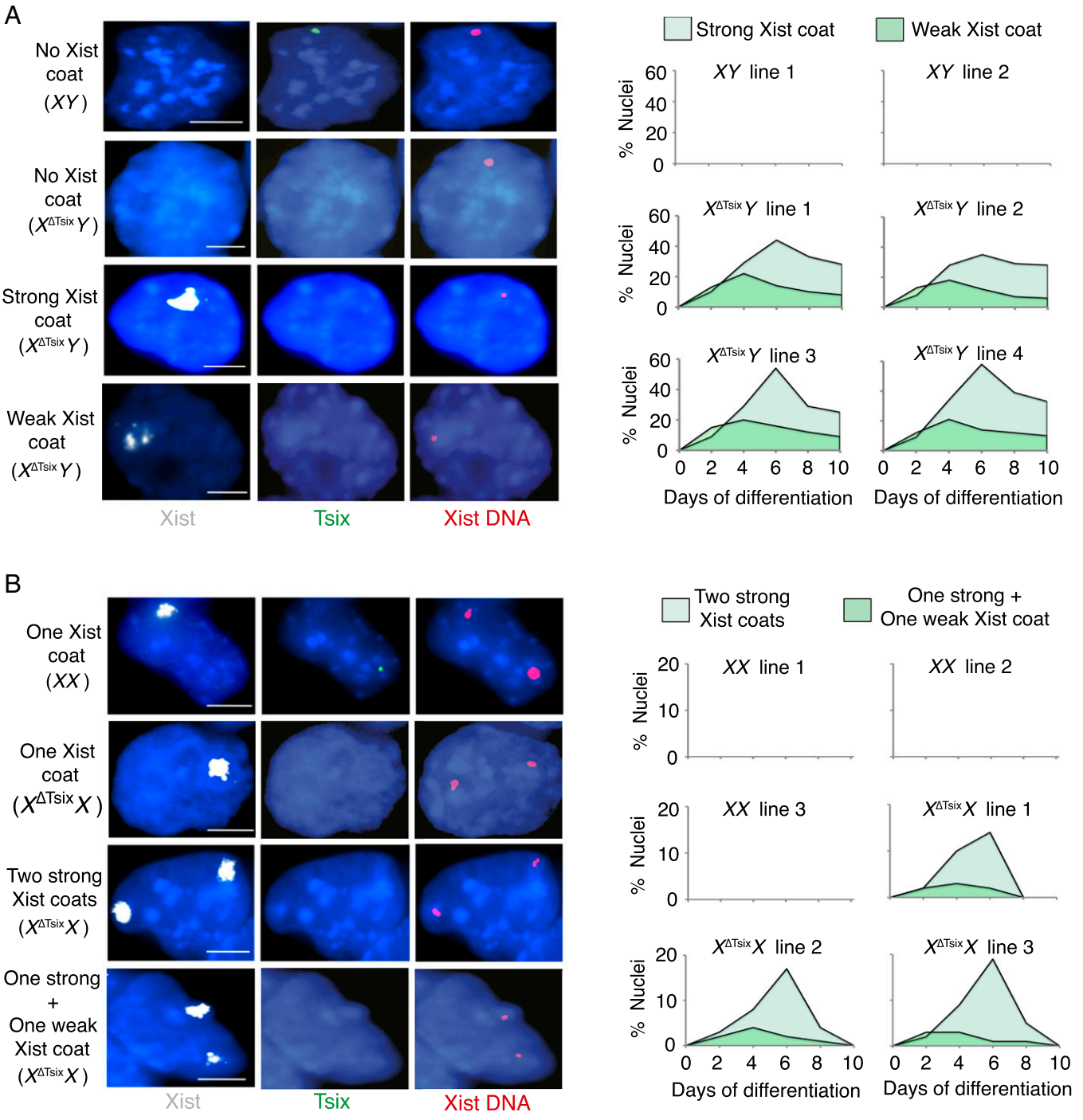

Fig. 1. Differential Xist RNA coating in $X^{\Delta Tsix}Y$ vs. $X^{\Delta Tsix}X$ differentiating ESCs. (*A*, *Left*) RNA FISH detection of Xist (white) and Tsix (green) RNAs followed by Xist DNA FISH (red) in representative *XY* and $X^{\Delta Tsix}Y$ differentiated ESCs without or with strong or weak Xist RNA coats. Nuclei are stained blue with DAPI. (*Right*) Quantification of nuclei with strong or weak Xist RNA coats during differentiation of two *XY* and four $X^{\Delta Tsix}Y$ ESC lines. (*B*, *Left*) Xist/Tsix RNA FISH followed by Xist DNA FISH in representative *XX* and $X^{\Delta Tsix}X$ differentiated ESCs. (*Right*) Quantification of nuclei with strong or weak ectopic Xist RNA coats during differentiation in three *XX* and three $X^{\Delta Tsix}X$ ESC lines. Only nuclei with a single Xist locus in males or two Xist loci in females detected by DNA FISH were quantified. n = 100 nuclei per cell line per day of differentiation. (Scale bar, 2 μm.) Related data are included in *SI Appendix*, Fig. S1.

upon differentiation (6, 30, 32). During the 10-d course of differentiation, *XX* cells either lacked Xist RNA coating, signifying that X inactivation had not yet initiated, or had one Xist RNA coat, characteristic of the inactive X. We did not observe WT *XX* nuclei with two Xist RNA coats throughout the time course. In contrast, differentiating mutant $X^{\Delta Tsix}X$ ESCs displayed two strong Xist-coated Xs in a significant percentage of $X^{\Delta Tsix}X$ nuclei, peaking at between 14% and 19% at d6. A small percentage of differentiating $X^{\Delta Tsix}X$ nuclei exhibited one strong and one weak Xist RNA-coated X chromosome, with a maximum of 4%. By d10, double Xist RNA-coated $X^{\Delta Tsix}X$ nuclei had rapidly declined and disappeared altogether (Fig. 1*B*), in marked contrast to the male $X^{\Delta Tsix}Y$ ESCs, which showed persistence of ectopic Xist RNA-coated nuclei (Fig. 1*A*). We previously showed that the second Xist-decorated X chromosome in differentiating $X^{\Delta Tsix}X$ ESCs is the $X^{\Delta Tsix}$ mutant X chromosome (30). Xist is therefore ectopically induced from the $X^{\Delta Tsix}$ in females, as it is in males. Compared with $X^{\Delta Tsix}Y$ ESCs, however, differentiating $X^{\Delta Tsix}X$ ESCs appeared to harbor fewer ectopic Xist RNA-decorated nuclei.

Sex-Specific X-Linked Gene Silencing upon Ectopic Xist RNA Coating in ESCs. We surmised that the difference in the frequency and the kinetics of ectopic Xist RNA-coated nuclei between male $X^{\Delta Tsix}Y$ and female $X^{\Delta Tsix}X$ ESC lines may reflect variable silencing of X-linked genes between the sexes. Functional nullizygosity of X-linked genes is expected to be deleterious, leading to selection against these cells (30, 33). Thus, the higher steady-state percentage of $X^{\Delta Tsix}Y$ nuclei with Xist RNA coating may reflect inefficient silencing of X-linked genes upon ectopic Xist RNA coating in mutant males compared with females.

To test the efficiency of X-linked gene silencing in $X^{\Delta Tsix}Y$ and $X^{\Delta Tsix}X$ cells, we profiled the expression of Xist RNA together with a panel of genes distributed across the X chromosome in differentiating WT and mutant ESCs by RNA FISH (Fig. 2*A*). RNA FISH permits detection of nascent transcripts in single cells and is refractory to potentially confounding variables of RNA perdurance and expression heterogeneity in and between cells to which techniques such as RT-PCR or RNA sequencing (RNA-seq) are subject. We assayed nine genes that are subject to X inactivation, *Lamp2*, *Mecp2*, *G6pdx*, *Chic1*, *Rnf12*, *Atrx*, *Pgk1*, *Gla*, and *Pdha1* (16, 34, 35). In differentiating WT male *XY* ESCs, all of the genes were expressed in most of the nuclei (61–94%) (Fig. 2*B* and *SI Appendix*, Fig. S2). In differentiating WT female *XX* ESCs, the nine genes were similarly monoallelically expressed (62–92%) (Fig. 2*B* and *SI Appendix*, Fig. S2). The remaining cells failed to display expression from the single allele in males or both alleles in females. As a control, we additionally assayed a gene that escapes X inactivation, *Smcx*, which is expected to be expressed from both the active and the inactive X in females. In *XY* cells, *Smcx* was expressed from the single X chromosome in ~90% of cells; in *XX* females, *Smcx* was biallelically expressed in ~60% of the cells (*SI Appendix*, Fig. S2*B*).

In differentiating $X^{\Delta Tsix}Y$ male ESCs, we noticed that all genes were expressed in a significant percentage of nuclei despite strong Xist RNA coating (Fig. 2*B* and *SI Appendix*, Fig. S2*B*). In nuclei with weak Xist RNA coating, all of the genes were expressed more often from the $X^{\Delta Tsix}$ compared with nuclei with strong Xist RNA coating (*SI Appendix*, Figs. S2*B* and S3*A*). By contrast, in differentiating $X^{\Delta Tsix}X$ female ESCs with two strong Xist RNA coats, all X-linked genes were silenced on both Xs in significantly more nuclei than in strong Xist RNA-decorated $X^{\Delta Tsix}Y$ male nuclei (Fig. 2*B* and *SI Appendix*, Figs. S2*B*, S3*A*, and Table S1). In $X^{\Delta Tsix}X$ female nuclei with one strong and one weak Xist RNA coat, all X-linked genes were coincidently expressed with Xist RNA in a greater percentage than in $X^{\Delta Tsix}X$ nuclei with two strong Xist RNA coats (Fig. 2*B* and *SI Appendix*, Figs. S2*B* and S3*A*). However, X-linked genes were silenced more often in female $X^{\Delta Tsix}X$ nuclei with one strong and one weak Xist RNA coat than in male $X^{\Delta Tsix}Y$ nuclei with a weak Xist RNA coat (*SI Appendix*, Figs. S2*B* and S3*A*). In summary,

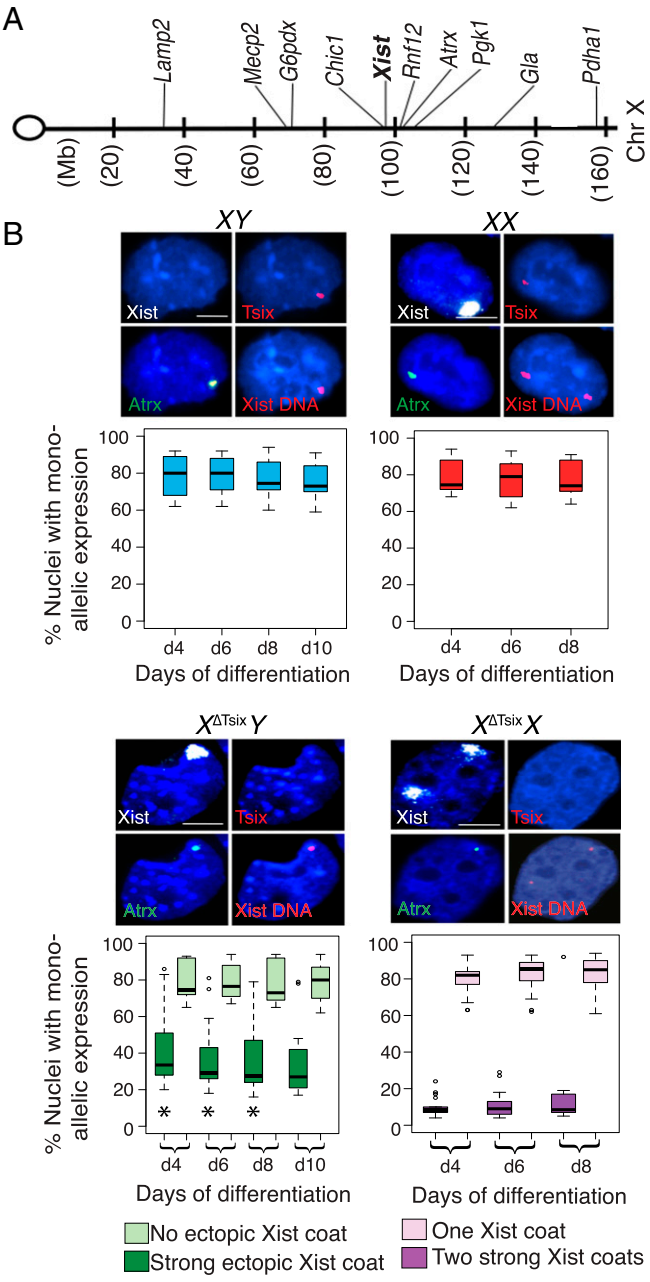

Fig. 2. Differential silencing of X-linked genes upon ectopic Xist RNA coating in differentiating $X^{\Delta Tsix}Y$ and $X^{\Delta Tsix}X$ ESCs. (*A*) X-chromosomal localization of the genes profiled by RNA FISH. (*B*) A representative nucleus stained to detect Xist RNA (white), Tsix RNA (red), and nascent transcripts of one of the nine genes surveyed (*Atrx*, green) is shown above boxplots of each genotype. Following RNA FISH, the Xist locus was detected by DNA FISH. Nuclei are stained blue with DAPI. Boxplots show the median percent gene expression (line), second to third quartiles (box), and 1.5 times the interquartile range (whiskers). d, day. In *XY* and *XX* cells, nuclei exhibiting monoallelic expression are plotted. In $X^{\Delta Tsix}Y$ cells, percent nuclei with monoallelic expression of the genes both without coincident Xist RNA coat and with strong ectopic Xist RNA coats are plotted. In $X^{\Delta Tsix}X$ cells, percent nuclei with monoallelic expression of the genes coincident with a single Xist RNA coat and with two strong ectopic Xist RNA coats are plotted. Two cell lines of each genotype were analyzed. $n = 100$ nuclei per cell line per day of differentiation for each class of Xist RNA-coated cells. (Scale bar, 2 μm.) $^*P < 0.003$, significant difference in gene expression between $X^{\Delta Tsix}Y$ and $X^{\Delta Tsix}X$ nuclei; Welch's two-sample *T* test. X-linked gene expression does not differ significantly between $X^{\Delta Tsix}Y$ and $X^{\Delta Tsix}X$ nuclei lacking ectopic Xist coats ($P > 0.2$). Related data are included in *SI Appendix*, Figs. S2 and S3.

compared with $X^{\Delta Tsix}Y$ male cells, differentiating $X^{\Delta Tsix}X$ female ESCs silenced all nine genes in significantly more nuclei upon ectopic Xist RNA coating. The weaker silencing in $X^{\Delta Tsix}Y$ males compared with $X^{\Delta Tsix}X$ females may underlie the increased prevalence of Xist RNA-decorated male cells relative to double Xist RNA-coated female cells later in differentiation. Upon ectopic Xist RNA coating, stringent silencing of genes on the second X chromosome potently selects against $X^{\Delta Tsix}X$ cells (see below and ref. 30); by contrast, weaker silencing of X-linked genes in $X^{\Delta Tsix}Y$ cells may permit Xist RNA-coated cells to persist.

Xist RNA is thought to potentiate silencing by directly or indirectly recruiting proteins such as the Polycomb group. Thus, as an added indicator of the potency of Xist RNA coating, we tested enrichment of histone H3 trimethylated at lysine 27 (H3-K27me3) on both the strong and weak Xist RNA-coated X chromosomes. H3-K27me3 is catalyzed by the Polycomb repressive complex 2 (PRC2) and is associated with silenced gene expression (36), including on the inactive X chromosome (37, 38). Whereas strong Xist RNA coats displayed robust coincident H3-K27me3 enrichment in both sexes (~90% of cells), a significant percentage of weak Xist RNA coats also showed overlapping H3-K27me3 enrichment (~75% of cells), albeit with correspondingly weaker signals in both sexes (*SI Appendix*, Fig. S3*B*). The reduced frequency of H3-K27me3 enrichment on the weak Xist RNA-coated Xs correlates with the weaker silencing of genes on that X chromosome in both sexes (*SI Appendix*, Fig. S3*B*). In sum, the reduced levels of X-linked gene silencing in $X^{\Delta Tsix}Y$ cells is not due to lower frequencies of H3-K27me3 enrichment on the Xist RNA-decorated Xs in comparison with $X^{\Delta Tsix}X$ cells.

Y Chromosome Does Not Protect Against X-Linked Gene Silencing in $X^{\Delta Tsix}Y$ ESCs. To explain the differential X-linked gene silencing in $X^{\Delta Tsix}Y$ vs. $X^{\Delta Tsix}X$ cells, we investigated whether the presence of the Y chromosome protected X-linked genes from being silenced. Previous studies have demonstrated that Xist RNA coating can occur in male ESCs with supernumerary X chromosomes (33), but, to our knowledge, whether silencing of individual genes can occur to the same extent in male cells as in corresponding cells without a Y chromosome is not known. We therefore subcloned two 39,$X^{\Delta Tsix}$ ($X^{\Delta Tsix}O$) ESC lines from $X^{\Delta Tsix}X$ ESCs (ESC line 2 in Fig. 1*B*) that have lost the WT X chromosome and assessed Xist RNA coating and expression of the 10 X-linked genes by RNA FISH. During differentiation, the frequency of strong and weak Xist RNA-coated nuclei in both of the $X^{\Delta Tsix}O$ ESC lines mimicked $X^{\Delta Tsix}Y$ ESCs and not $X^{\Delta Tsix}X$ ESCs, including the parental $X^{\Delta Tsix}X$ ESC line 2 (*SI Appendix*, Fig. S3*C*). Moreover, in both strong and weak Xist RNA-coated $X^{\Delta Tsix}O$ nuclei, the expression pattern of all 10 genes matched that of the $X^{\Delta Tsix}Y$ cells instead of the parental $X^{\Delta Tsix}X$ cells (*SI Appendix*, Figs. S2*B*, S3*D*, and Table S2). Thus, the absence of the Y chromosome does not explain the greater frequency of X-linked gene silencing in $X^{\Delta Tsix}X$ compared with $X^{\Delta Tsix}Y$ cells. The differential silencing between the sexes must therefore be dependent on the X-chromosomal content.

Sex-Specific Difference in Ectopic Xist RNA Coat Frequencies in EpiSCs. Female ESCs have two active X chromosomes; thus, the higher X-chromosomal dose necessary for efficient X-linked gene silencing could require both Xs to be transcriptionally active. Alternatively, higher X-chromosome dosage may have an effect even if one of the two Xs was inactivated. To distinguish among these two distinct possibilities, we took advantage of Tsix-mutant EpiSCs. Like ESCs, EpiSCs are pluripotent cells of the epiblast lineage (39, 40). However, as opposed to ESCs, undifferentiated female EpiSCs, *XX* as well as $X^{\Delta Tsix}X$, harbor a stochastically inactivated X chromosome (30, 41, 42).

We first profiled Xist RNA coating in WT and mutant EpiSCs. Male WT *XY* as well as mutant $X^{\Delta Tsix}Y$ EpiSCs did not display Xist RNA coating in the undifferentiated state (Fig. 3*A* and *SI Appendix*, Fig. S4*A*). WT *XY* male cells remained devoid of Xist RNA coating throughout differentiation; differentiating mutant $X^{\Delta Tsix}Y$ male cells, however, exhibited a significant percentage with Xist RNA coats (Fig. 3*A* and *SI Appendix*, Fig. S4*A*). Undifferentiated *XX* and $X^{\Delta Tsix}X$ female EpiSCs were also indistinguishable. Both genotypes displayed a single Xist RNA-coated X chromosome (Fig. 3*B* and *SI Appendix*, Fig. S4*B*) (30). Upon differentiation, however, a proportion of $X^{\Delta Tsix}X$ female EpiSCs ectopically induced Xist and coated the second X chromosome (Fig. 3*B* and *SI Appendix*, Fig. S4*B*); *XX* female EpiSCs continued to exhibit only one Xist RNA coat during the course of differentiation. Xist decoration of the second X chromosome in $X^{\Delta Tsix}X$ female cells is due to ectopic Xist induction from the $X^{\Delta Tsix}$, as in $X^{\Delta Tsix}Y$ male cells (30).

Like ESCs, the mutant EpiSCs displayed a sex-specific pattern of Xist RNA coating. In differentiating $X^{\Delta Tsix}Y$ male EpiSCs, the percentage of strong Xist RNA-coated nuclei steadily increased up to d20 of differentiation, ranging between 42% and 59% of nuclei, then decreased to between 22% and 26% at d30 (Fig. 3*A*). Weak Xist RNA-coated $X^{\Delta Tsix}Y$ male nuclei peaked

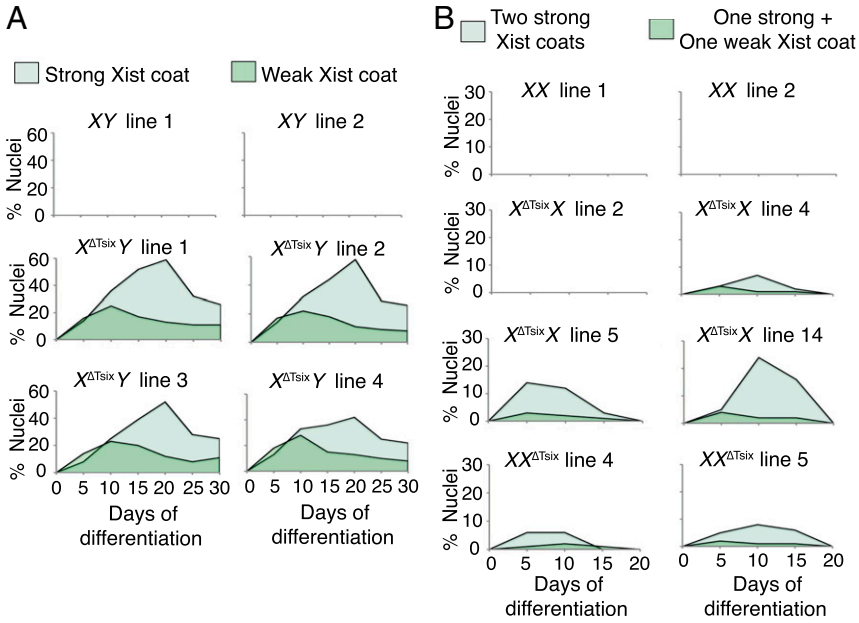

Fig. 3. Differential ectopic Xist RNA coating in differentiating $X^{\Delta Tsix}Y$ vs. $X^{\Delta Tsix}X$ EpiSCs. (*A*, *Left*) Quantification of nuclei with strong or weak Xist RNA coats during differentiation of two *XY* and four $X^{\Delta Tsix}Y$ EpiSC lines. (*B*, *Right*) Quantification of nuclei with strong or weak ectopic Xist RNA coats during differentiation of two *XX* and six $X^{\Delta Tsix}X$ EpiSC lines. Only nuclei with a single Xist locus in males or two Xist loci in females detected by DNA FISH were quantified, as shown in *SI Appendix*, Fig. S4. $n = 100$ nuclei per cell line per day of differentiation.

between 22% and 28%, at d10, and decreased to 8–11% at d30 (Fig. 3*A*). By contrast, the percentage of $X^{\Delta Tsix}X$ female nuclei with strong ectopic Xist RNA coating, resulting in two robust Xist RNA-decorated domains, reached a maximum of 24% at d10 and then quickly disappeared by d20 (Fig. 3*B*). $X^{\Delta Tsix}X$ nuclei with one strong and one weak Xist RNA coats peaked at 4% at d5–d10 and were gone by d20.

The variability in ectopic Xist induction between the female EpiSC lines roughly correlates with the number of cells that are eligible to ectopically induce Xist in a given line. Due to random X inactivation, $X^{\Delta Tsix}X$ EpiSCs can inactivate either the mutant $X^{\Delta Tsix}$ or the WT X (30). The greater the percentage of cells in a female EpiSC line in which the $X^{\Delta Tsix}$ is the active X, the higher the percentage of cells that can ectopically express Xist (30). For example, in $X^{\Delta Tsix}X$ EpiSC line 2 the $X^{\Delta Tsix}$ is the inactive X in all cells; this cell line, therefore, entirely lacks cells that can ectopically induce Xist, in agreement with the absolute absence of nuclei with two Xist RNA coats in this cell line during differentiation (Fig. 3*B*). Conversely, $X^{\Delta Tsix}X$ EpiSC line 14 harbors many cells that have chosen the $X^{\Delta Tsix}$ as the active X chromosome (~75%), resulting in a relatively high percentage of cells that ectopically induce Xist during differentiation (Fig. 3*B*). Nevertheless, even in this cell line substantially fewer nuclei displayed ectopic Xist RNA coating (24%) compared with the $X^{\Delta Tsix}Y$ EpiSC line with the lowest frequency of ectopic Xist RNA-coated nuclei (cell line 4; 41%). This difference once again suggested diminished silencing of X-linked genes in mutant males compared with females.

Sex-Specific X-Linked Gene Silencing upon Ectopic Xist RNA Coating in EpiSCs. We therefore assayed expression of the 10 X-linked genes over the course of EpiSC differentiation by RNA FISH (Fig. 4 and *SI Appendix*, Fig. S5). Similarly to ESCs, significantly more differentiating mutant $X^{\Delta Tsix}X$ female compared with mutant $X^{\Delta Tsix}Y$ male EpiSCs exhibited silencing of the 9 genes subject to X inactivation upon ectopic Xist RNA coating ($P < 10^{-6}$; Fig. 4 and *SI Appendix*, Fig. S5 and Table S3). We also simultaneously probed pairs of X-linked genes to determine if in the same nucleus the expression of the two genes would concord, or, as implied by the data in *SI Appendix*, Fig. S5, differ. We tested four different pairs, with 1 gene of each pair exhibiting a greater frequency of silencing than the other when tested individually in $X^{\Delta Tsix}Y$ cells (*Pgk1*/*Atrx*; *Rnf12*/*Lamp2*; *Gla*/*Mecp2*; *G6pdx*/*Chic1*) (*SI Appendix*, Figs. S5 and S6). When tested together, the genes in each pair recapitulated the pattern of silencing when assayed individually in both $X^{\Delta Tsix}Y$ and $X^{\Delta Tsix}X$ cells (*SI Appendix*, Fig. S5). One gene was silenced more frequently compared with the other, especially in $X^{\Delta Tsix}Y$ cells; thus, the two genes behaved independently in the same nucleus. Notably, 7 of 8 genes were silenced in significantly more $X^{\Delta Tsix}X$ compared with $X^{\Delta Tsix}Y$ nuclei ($P < 0.03$; *Pgk1*, $P < 0.12$) (*SI Appendix*, Fig. S6). Thus, ectopic Xist RNA coating is sufficient to silence X-linked genes in $X^{\Delta Tsix}Y$ cells; but, it does not do so as uniformly or as robustly as in $X^{\Delta Tsix}X$ cells.

We also measured the ability of ectopic Xist RNA coating to recruit the Polycomb PRC2 complex and enrich H3-K27me3 on the X chromosome in differentiating EpiSCs. As in ESCs, both strong and weak Xist coats displayed accumulation of H3-K27me3 in a significant percentage of $X^{\Delta Tsix}Y$ and $X^{\Delta Tsix}X$ nuclei in both sexes (~90%, strong Xist-coated nuclei; ~75%, weak Xist-coated nuclei) (*SI Appendix*, Fig. S7). Concurrent detection of H3-K27me3, Xist, and X-linked genes directly showed that despite the robust enrichment of H3-K27me3 on the ectopically Xist-coated $X^{\Delta Tsix}$, X-linked genes were nevertheless expressed in a significant percentage of differentiating male $X^{\Delta Tsix}Y$ EpiSCs ($P < 0.001$; *SI Appendix*, Fig. S8). Furthermore, consistent with the relatively stringent silencing upon ectopic Xist RNA coating in differentiating $X^{\Delta Tsix}X$ compared with $X^{\Delta Tsix}Y$ cells, mutant female cells displayed a significant reduction in both cell proliferation and viability compared with mutant male cells during differentiation ($P < 10^{-4}$) (*SI Appendix*, Fig. S9; see also ref. 30). Reduced proliferation and increased cell death, therefore, potently select against female mutants that have ectopically activated Xist from and silenced genes on the second, i.e., $X^{\Delta Tsix}$, X chromosome.

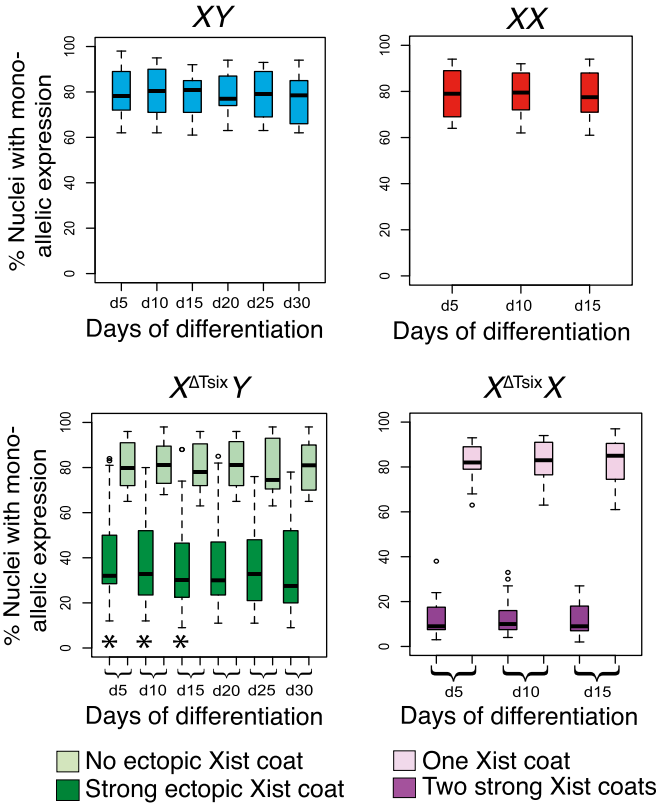

Fig. 4. Differential silencing of X-linked genes upon ectopic Xist RNA coating in differentiating $X^{\Delta Tsix}Y$ vs. $X^{\Delta Tsix}X$ EpiSCs. Boxplots of expression of the nine X-linked genes surveyed as in Fig. 2 in individual nuclei of differentiating *XY*, *XX*, $X^{\Delta Tsix}Y$, and $X^{\Delta Tsix}X$ EpiSC lines (lines 2, 2, 4, and 5, respectively; all EpiSC lines from Fig. 3, with the exception of $X^{\Delta Tsix}X$ EpiSC line 2). d, day. $n = 100$ nuclei per cell line per day of differentiation for each class of Xist RNA-coated cells. *$P < 10^{-6}$, significant difference in gene expression between $X^{\Delta Tsix}Y$ and $X^{\Delta Tsix}X$ nuclei; Welch's two-sample *T* test. X-linked gene expression does not significantly differ between $X^{\Delta Tsix}Y$ and $X^{\Delta Tsix}X$ nuclei lacking ectopic Xist coats ($P > 0.2$). Related data are included in *SI Appendix*, Figs. S5–11.

In summary, the sex-specific pattern of ectopic Xist induction and X-linked gene silencing occurs in differentiating EpiSCs, as it does in ESCs. Thus, robust silencing of X-linked genes does not require two transcriptionally active Xs and can occur even when one of the two Xs in females is inactivated.

Equivalent Levels of Ectopic Xist Expression in Individual $X^{\Delta Tsix}Y$ vs. $X^{\Delta Tsix}X$ EpiSCs. In principle, the sex-specific X-linked gene silencing may be due to lower levels of ectopic Xist RNA expression in $X^{\Delta Tsix}Y$ compared with $X^{\Delta Tsix}X$ cells. We therefore sought to quantify Xist expression in male and female mutant EpiSCs. We took advantage of a single nucleotide polymorphism (SNP) that distinguishes Xist transcripts originating from the $X^{\Delta Tsix}$ vs. the WT X chromosome via pyrosequencing of cDNAs. Whereas the $X^{\Delta Tsix}$ is derived from a *M. musculus* strain, the WT X is derived from the divergent *M. molossinus* JF1 strain (X^{JF1}). We first measured Xist expression in $X^{\Delta Tsix}Y$ males relative to a reference F1 hybrid female EpiSC line, $X^{\Delta Tsix}X^{JF1}$ line 15, in which Xist is predominantly expressed from the X^{JF1} (30). Due to the variability in Xist induction between cells, we profiled Xist expression in individual cells. In the $X^{\Delta Tsix}X^{JF1}$ EpiSC line 15, Xist was almost exclusively expressed from the WT X^{JF1} allele (>90% of total Xist expression) in all cells examined (*SI Appendix*, Fig. S10*A*). By contrast, in single WT F1 hybrid $X^{JF1}X^{Lab}$ EpiSCs, in

which the X^{Lab} is *M. musculus* derived, Xist was nearly mutually exclusively expressed from either the X^{JF1} or the X^{Lab} (*SI Appendix*, Fig. S10*B*), consistent with stochastic inactivation of either X chromosome in individual cells.

To quantify Xist expression in $X^{\Delta Tsix}Y$ male EpiSCs, we combined single $X^{\Delta Tsix}Y$ cells (line 3 in Fig. 3*A*) with single $X^{\Delta Tsix}X^{JF1}$ line 15 female EpiSCs. Consistent with the lack of Xist RNA coating in undifferentiated $X^{\Delta Tsix}Y$ EpiSCs by RNA FISH (Fig. 3*A*), when single undifferentiated $X^{\Delta Tsix}Y$ EpiSCs were combined with single undifferentiated $X^{\Delta Tsix}X^{JF1}$ line 15 EpiSCs, Xist expression from the $X^{\Delta Tsix}$ did not increase compared with undifferentiated $X^{\Delta Tsix}X^{JF1}$ line 15 EpiSCs alone (*SI Appendix*, Fig. S10*C*). Upon differentiation, based on the RNA FISH data we expected to observe three classes of $X^{\Delta Tsix}Y$ cells by RT-PCR (*SI Appendix*, Fig. S10*D*). In the first, the cells would be devoid of Xist induction or induced Xist minimally. In the second, Xist would be moderately expressed, thus corresponding to the weak Xist RNA-coated cells by RNA FISH. In the third, Xist would be strongly induced, representing robust Xist RNA-decorated cells. When single d10 differentiated $X^{\Delta Tsix}Y$ EpiSCs were combined with single undifferentiated line 15 female EpiSCs, Xist expression from the $X^{\Delta Tsix}$ increased in a substantial percentage of the samples (*SI Appendix*, Fig. S10*E*), in agreement with Xist induction in some but not all $X^{\Delta Tsix}Y$ cells by RNA FISH (Fig. 3*A*). Of the three categories, class I cells, which did not induce Xist or induced Xist minimally (≤10% of total Xist expression from the $X^{\Delta Tsix}$), accounted for 31% of all cells. Class II cells, which induced Xist moderately (30–39% of total Xist expression from the $X^{\Delta Tsix}$), represented 28% of the cells. We chose 40% as the threshold of expression from the $X^{\Delta Tsix}$ between class II and class III (robust Xist induction from the $X^{\Delta Tsix}$) because in individual differentiating $X^{\Delta Tsix}X$ female cells, robust ectopic Xist induction from the $X^{\Delta Tsix}$ X chromosome yields values of >40% (see below). The strong Xist-expressing class III cells (40–68% of total Xist expression from the $X^{\Delta Tsix}$) were 41% of the total cells. In class III $X^{\Delta Tsix}Y$ cells, the average Xist expression from the $X^{\Delta Tsix}$ was 57% of total. This level of Xist induction in $X^{\Delta Tsix}Y$ male cells matched Xist expression from the $X^{\Delta Tsix}$ in females, measured by combining single cells from female EpiSC lines that express Xist almost exclusively from either the $X^{\Delta Tsix}$ ($X^{\Delta Tsix}X^{JF1}$ EpiSC line 2) or the X^{JF1} ($X^{\Delta Tsix}X^{JF1}$ EpiSC line 15) (30), with an average of 58% of total Xist expression from the $X^{\Delta Tsix}$ (*SI Appendix*, Fig. S10*F*). The higher Xist expression from the $X^{\Delta Tsix}$ relative to X^{JF1} reflects strain-specific differences in Xist levels due to polymorphisms in the X-controlling element (*Xce*) (43–45).

To gauge ectopic Xist induction later in differentiation, we also similarly profiled d20 differentiated $X^{\Delta Tsix}Y$ EpiSCs, when the percentage of Xist-coated cells is at its highest (Fig. 3*A*). By d20, class I accounted for 19% of all cells, class II 12%, and class III 69% (*SI Appendix*, Fig. S10*G*). As with robust Xist-expressing class III cells at d10, on average the d20 class III cells expressed Xist from the $X^{\Delta Tsix}$ at nearly the levels found in females in *SI Appendix*, Fig. S10*F* (59% vs. 58%). Of note, at both d10 and d20, a greater percentage of $X^{\Delta Tsix}Y$ cells strongly induced Xist (class III) relative to those with robust Xist RNA coats (41% vs. 25% at d10; 69% vs. 52% at d20) (*SI Appendix*, Fig. S10 *E*–*G* and Fig. 3*A*), suggesting that not all strong Xist expressers display robust Xist RNA coats. The percentage of class II cells with moderate Xist induction more closely approximated the percentage of nuclei displaying weak Xist RNA coats at d10 and at d20 (28% vs. 23% at d10; 19% vs. 12% at d20).

To quantify ectopic Xist expression in mutant females, we used an F1 hybrid $X^{\Delta Tsix}X^{JF1}$ female EpiSC line that exhibits ectopic Xist RNA coating of the $X^{\Delta Tsix}$ in a significant percentage of cells at d10 of differentiation (22%; $X^{\Delta Tsix}X$ EpiSC line 14 in Fig. 3*B*). Undifferentiated line 14 $X^{\Delta Tsix}X^{JF1}$ EpiSCs displayed a slightly biased pattern of X inactivation; two-thirds of the individual undifferentiated cells surveyed displayed Xist induction from the X^{JF1} X chromosome and one-third from the $X^{\Delta Tsix}$ X chromosome (*SI Appendix*, Fig. S10*H*). This distribution was expected to change during differentiation based on the RNA FISH data (Fig. 3*B*; see also ref. 30), with the cells once again expected to be stratified into three classes (*SI Appendix*, Fig. S10*I*). Class I would express Xist exclusively or almost exclusively from the X^{JF1} and lack much ectopic Xist induction from the $X^{\Delta Tsix}$ due to the lack of differentiation. Class II would correspond to cells that originally inactivated the WT X^{JF1} and robustly ectopically induced Xist from the $X^{\Delta Tsix}$ during differentiation. Class III represents cells that initially inactivated the $X^{\Delta Tsix}$ and therefore are not eligible to ectopically induce Xist from the second X (i.e., the WT X^{JF1}); these cells would therefore only express Xist from the $X^{\Delta Tsix}$ throughout differentiation. At d10 of differentiation, class I (≤10% of total Xist expression from the $X^{\Delta Tsix}$) accounted for 18% of the cells; class II (48–66% of total Xist expression from the $X^{\Delta Tsix}$) represented 23% of all cells; and class III (≥90% of total Xist expression from the $X^{\Delta Tsix}$), 59% of the cells (*SI Appendix*, Fig. S10*J*). Class II female cells, therefore, are most informative with respect to ectopic Xist induction, because only this group of cells expresses both Xist alleles. Notably, ectopic Xist expression in $X^{\Delta Tsix}X^{JF1}$ females is almost always robust, consistent with RNA FISH detecting very few mutant female nuclei with weak ectopic Xist coats (<4%) during EpiSC differentiation (Fig. 3*B*). The average expression of the two Xist alleles in individual class II cells was 57% from the $X^{\Delta Tsix}$ and 43% from the X^{JF1} X chromosome (*SI Appendix*, Fig. S10*J*). This distribution matched allelic Xist expression in single-cell mixtures of female EpiSCs that display preferential inactivation of either the $X^{\Delta Tsix}$ or the X^{JF1} (58% from the $X^{\Delta Tsix}$; 42% from the X^{JF1}) (*SI Appendix*, Fig. S10*F*). Moreover, class II percentage (23%) agrees well with the percentage of cells displaying two Xist RNA coats in this EpiSC line at d10 of differentiation by RNA FISH (22%) (Fig. 3*B*). Thus, in both $X^{\Delta Tsix}Y$ and $X^{\Delta Tsix}X$ EpiSCs, the $X^{\Delta Tsix}$ is able to ectopically induce Xist at levels matching Xist normally expressed from the WT inactive X in females.

By d20 of differentiation, $X^{\Delta Tsix}X^{JF1}$ cells only exhibited Xist RNA originating from the $X^{\Delta Tsix}$ (*SI Appendix*, Fig. S10*K*). The uniform expression of Xist from the $X^{\Delta Tsix}$ is consistent with selection against cells that had originally inactivated the X^{JF1}. During differentiation, all of these cells ectopically induced Xist robustly from the previously active $X^{\Delta Tsix}$ and became deficient in X-linked gene expression (Figs. 3*B* and 4 and *SI Appendix*, Fig. S5), leading to reduced proliferation and induced cell death (*SI Appendix*, Fig. S9) (see also ref. 30). By contrast, a significant fraction of male $X^{\Delta Tsix}Y$ d20 differentiated cells either failed to induce Xist (19%) or induced Xist only moderately (12%) (*SI Appendix*, Fig. S10*G*). And, at d10, when some differentiating female $X^{\Delta Tsix}X^{JF1}$ cells had not yet ectopically induced Xist, a greater percentage of $X^{\Delta Tsix}Y$ compared with $X^{\Delta Tsix}X$ cells either lacked ectopic Xist induction (31% vs. 18%) or induced Xist moderately (28% vs. 0%) (*SI Appendix*, Fig. S10 *E* and *J*).

Equivalent Ectopic Xist RNA Coating in $X^{\Delta Tsix}Y$ vs. $X^{\Delta Tsix}X$ EpiSCs. Although Xist RNA can be equivalently robustly expressed between the sexes, reduced Xist RNA coating could explain the diminished frequency of X-linked gene silencing in differentiated $X^{\Delta Tsix}Y$ compared with $X^{\Delta Tsix}X$ cells. We therefore quantified the volume as well as the intensity of the Xist RNA coats in $X^{\Delta Tsix}Y$, $X^{\Delta Tsix}X$, and *XX* EpiSCs, using an automated voxel-based analysis (*Materials and Methods*). We focused these measurements on nuclei with strong Xist RNA coats quantified in Figs. 3 and 4. Neither the volume nor the intensity of the Xist RNA coats was significantly different between male and female mutants (*SI Appendix*, Fig. S11). Moreover, neither measurement correlated with silencing of the five X-linked genes tested (*Lamp2*, *Mecp2*, *Atrx*, *Gla*, and *Pdha1*) (*SI Appendix*, Fig. S11); cells that expressed the X-linked genes did not have smaller or less intense coats compared with cells in which the genes were silenced. Together, these data demonstrate that, in EpiSC nuclei with robust ectopic Xist RNA coating, the strength of the Xist RNA coats in differentiating $X^{\Delta Tsix}Y$ is equivalent to that of $X^{\Delta Tsix}X$ EpiSCs. The difference in X-linked gene silencing between

the sexes, therefore, is not due to weaker Xist RNA coating in $X^{\Delta Tsix}Y$ compared with $X^{\Delta Tsix}X$ cells.

Embryos Display Sex-Specific Differences in Ectopic Xist Induction and X-Linked Gene Silencing. We next interrogated Tsix-mutant embryonic epiblasts to test whether the sex-specific pattern of Xist induction and X-linked silencing observed in differentiating ESCs and EpiSCs is also observed in vivo. We first assayed the percentage of ectopic Xist RNA-coated epiblast cells from embryonic day 5.5 (E5.5), E6.5, E7.5, E8.5, and E9.5 $X^{\Delta Tsix}Y$ male and $X^{\Delta Tsix}X$ female embryos. In $X^{\Delta Tsix}Y$ male embryos, a significant percentage of epiblast nuclei of E5.5 embryos, a stage shortly after random X-inactivation initiates (30, 46), exhibited ectopic Xist RNA coating (39%), which decreased at E6.5 (30%) and continued declining thereafter but were still found at E9.5 (Fig. 5*A*). In $X^{\Delta Tsix}X$ embryos, ectopic Xist RNA-coated epiblast nuclei with two Xist RNA coats were almost exclusively observed at E5.5 (22%), with very few at E6.5 (3%), and none at the later stages (Fig. 5*B*). Thus, $X^{\Delta Tsix}Y$ and $X^{\Delta Tsix}X$ embryos also display the sex-specific pattern of ectopic Xist induction observed in ESCs and EpiSCs. The difference in the kinetics of ectopic Xist induction in embryos compared with ESCs and EpiSCs reflects the relatively rapid rate of differentiation of embryonic epiblasts (30).

We next probed pairs of X-linked genes to test whether they were concordantly or discordantly silenced in individual embryonic nuclei upon ectopic Xist RNA coating in Tsix-mutant E5.5 and E6.5 epiblast cells of both sexes, as in the EpiSCs (*SI Appendix*, Fig. S6). The X-linked genes were variably silenced within and between the sexes, with a greater average frequency of silencing in $X^{\Delta Tsix}X$ females compared with $X^{\Delta Tsix}Y$ males (Fig. 5*C*). For three pairs of genes exhibiting differential levels of silencing (*Atrx*/*Pgk1*; *Lamp2*/*Rnf12*; *Mecp2*/*Gla*), one gene of each pair was silenced significantly less often than the other gene in the pair in $X^{\Delta Tsix}Y$ nuclei ($P < 0.05$), as compared to the $X^{\Delta Tsix}X$ nuclei (*SI Appendix*, Fig. S12), consistent with the EpiSC results (*SI Appendix*, Fig. S6). The fourth gene pair, *G6pdx*/*Chic1*, was rarely discordantly silenced in either sex. At E5.5, for six of the eight genes tested significantly fewer $X^{\Delta Tsix}Y$ male nuclei displayed silencing of the X-linked genes compared with $X^{\Delta Tsix}X$ female nuclei upon ectopic Xist coating ($P < 0.01$); only silencing of *Pgk1* and *Rnf12* did not differ significantly between the sexes ($P > 0.05$) (*SI Appendix*, Fig. S12). Similarly, at E6.5, upon ectopic Xist RNA coating all X-linked genes except *Pgk1* and *Rnf12* were silenced in significantly fewer $X^{\Delta Tsix}Y$ compared with $X^{\Delta Tsix}X$ nuclei ($P < 0.05$).

Discussion

Xist RNA is believed to be both necessary and sufficient to initiate X inactivation. To test Xist function, in this study we analyzed differentiating ESCs, EpiSCs, and embryonic epiblast cells harboring a mutation in the Xist antisense repressor Tsix. The $X^{\Delta Tsix}$ X chromosome offered a sensitized background in which to assess the impact of Xist RNA on X-linked gene silencing, because Xist is ectopically induced from the active $X^{\Delta Tsix}$ in the epiblast lineage of both males and females. We found that a higher frequency of $X^{\Delta Tsix}Y$ and $X^{\Delta Tsix}O$ cells displayed ectopic Xist RNA coating compared with $X^{\Delta Tsix}X$ cells. This increase reflected the inability of $X^{\Delta Tsix}Y$ and $X^{\Delta Tsix}O$ cells to efficiently silence X-linked genes upon ectopic Xist induction. Silencing of genes on both Xs due to ectopic Xist induction from the $X^{\Delta Tsix}$ resulted in significantly reduced proliferation and increased cell death in $X^{\Delta Tsix}X$ female cells relative to $X^{\Delta Tsix}Y$ male cells. The rapid loss of this population of $X^{\Delta Tsix}X$ female cells leaves behind only cells or descendants of cells that had originally inactivated the $X^{\Delta Tsix}$ and which could not induce Xist from the second, i.e., WT, X chromosome during differentiation (see also ref. 30). Therefore, despite a lower steady-state frequency of ectopic Xist RNA coating, all $X^{\Delta Tsix}X$ female mutant cells in which the $X^{\Delta Tsix}$ was the active X ultimately ectopically induce Xist from the $X^{\Delta Tsix}$. By contrast, a significant percentage of differentiating $X^{\Delta Tsix}Y$ male mutant epiblast cells do not induce Xist. Thus, $X^{\Delta Tsix}Y$ mutants not only display lower frequencies of X-linked gene silencing upon ectopic Xist induction, but also exhibit a reduced number of cells with ectopic Xist induction compared with $X^{\Delta Tsix}X$ female cells.

The X-chromosome:autosome ratio determines whether X inactivation occurs and how many X chromosomes undergo inactivation,

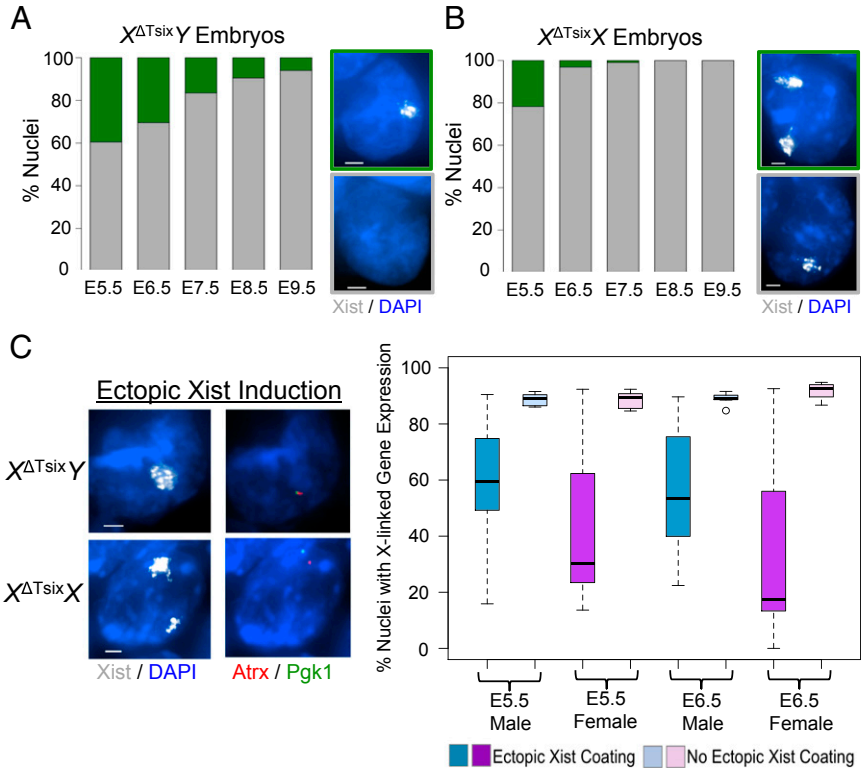

Fig. 5. Ectopic Xist induction and X-linked gene silencing in postimplantation $X^{\Delta Tsix}Y$ and $X^{\Delta Tsix}X$ embryos. (*A*) Quantification of $X^{\Delta Tsix}Y$ E5.5–E9.5 embryonic nuclei with and without Xist RNA coats. (*B*) Quantification of $X^{\Delta Tsix}X$ E5.5–E9.5 embryonic nuclei with one and two Xist RNA coats. (*C*) Analysis of expression of the X-linked genes *Lamp2*, *Mecp2*, *G6pdx*, *Chic1*, *Rnf12*, *Atrx*, *Pgk1*, and *Gla* in $X^{\Delta Tsix}Y$ and $X^{\Delta Tsix}X$ E5.5 and E6.5 embryonic epiblasts by RNA FISH. (*Left*) Representative images of nuclei stained to detect Xist, Atrx, and Pgk1 RNAs. (Scale bar, 2 μm.) (*Right*) Boxplots of expression of all eight X-linked genes surveyed. Boxplots show the median percent gene expression (line), second to third quartiles (box), and 1.5 times the interquartile range (whiskers). Related data are included in *SI Appendix*, Fig. S12.

ensuring that only one X remains active per diploid genome (47–51). In the Tsix mutants, the differences in Xist induction and X-linked gene silencing must be genetically attributed to the sex chromosomes, as both $X^{\Delta Tsix}X$ and $X^{\Delta Tsix}Y$ cells have identical complements of autosomes. Because differentiating $X^{\Delta Tsix}O$ ESCs behave similarly to $X^{\Delta Tsix}Y$ ESCs, we exclude the Y chromosome as the source of the sex-specific differences by, for example, Y-linked genes functioning to prevent X-linked gene silencing in males. Instead, the data implicate the presence of the second X chromosome—i.e., the WT X—as the cause of the increased frequencies of ectopic Xist induction and X-linked gene silencing in females compared with males.

In addition to truncating Tsix transcription, the ΔTsix mutation deletes the critical *DXPas34* repeat sequence close to the Xist–Tsix topological associated domain (TAD) boundary (30, 31, 52–56). Consistent with the broadly coordinated regulation of genes within each of the two adjacent TADs, a 58-kb deletion encompassing the TAD boundary changes the transcription of multiple genes within the *X-inactivation center* (*Xic*) (33, 57, 58). The ΔTsix mutation may result in a similar long-range dysregulation of X-linked genes *in cis* by perturbing the Xist–Tsix TAD boundary. However, the requirement for the second X chromosome implies that the observed sex-specific differences are a *trans*-effect, rather than due to a *cis*-limited sex-specific transcriptional defect on the $X^{\Delta Tsix}$ imparted by the ΔTsix mutation.

Another potential explanation for the sex-specific effects is differential epigenetic marking of the $X^{\Delta Tsix}$ in the two sexes. In females, the second X chromosome may alter the $X^{\Delta Tsix}$ chromatin in a manner that later facilitates ectopic Xist induction from and X-linked gene silencing on the $X^{\Delta Tsix}$. The observation that $X^{\Delta Tsix}O$ ESCs, which were derived from $X^{\Delta Tsix}X$ female ESCs and thus previously harbored two Xs, ectopically induce Xist and undergo X-linked gene silencing at frequencies similar to $X^{\Delta Tsix}Y$ male ESCs suggests that the presence of two active X chromosomes does not mark the $X^{\Delta Tsix}$ differently in females compared with males. Further arguing against such epigenetic differences is the propensity of $X^{\Delta Tsix}X$ ESCs to undergo random X inactivation, a pattern similar to that of WT *XX* cells (30). If the $X^{\Delta Tsix}$ was especially prone to inducing Xist and undergoing inactivation in females, the expectation is that it would preferentially be chosen for inactivation in $X^{\Delta Tsix}X$ heterozygotes.

Developmental differences between male and female embryos may also explain the sex-specific differences in Xist induction and X-linked gene silencing in the Tsix mutants. *XY* male embryos develop slightly faster compared with their *XX* siblings, owing both to the absence of the Y chromosome and the presence of the second X chromosome (59). Moreover, previous observations have suggested that Xist RNA is competent to silence X-linked genes in a defined developmental window (26). If cells in male embryos exceed this developmental window due to their faster development, then they may become refractory to X inactivation. Several observations, however, argue against the faster development of male embryos underlying the lower frequencies of X-linked gene silencing in $X^{\Delta Tsix}Y$ compared with $X^{\Delta Tsix}X$ embryos. For example, any difference in the rate of development of embryonic epiblasts between the sexes at E5.25 is not expected to be as large as the difference between E5.25 and E6.5 epiblasts. E6.5 epiblasts harbor more than five times the number of cells as in E5.25 epiblasts (60, 61). Upon ectopic Xist RNA coating, epiblasts in E6.5 $X^{\Delta Tsix}X$ females silenced each of the eight genes surveyed significantly more frequently than did E5.25 $X^{\Delta Tsix}Y$ males. Thus, female embryos older by >1 d are nevertheless more competent to silence X-linked genes than their younger male counterparts.

Cultured $X^{\Delta Tsix}Y$ and $X^{\Delta Tsix}X$ ESCs and EpiSCs recapitulate the sex-specific patterns observed in embryos, also arguing against developmental timing differences as the underlying cause of the sex-specific differences. Any developmental timing differences would be normalized by capturing cells of both sexes at equivalent stages of differentiation. Ectopic Xist induction and X-linked gene silencing occur at the same stage of ESC differentiation in both sexes (30). Xist is ectopically induced just after the ESCs differentiate beyond the epiblast-like cell (EpiLC) stage in both sexes (30). EpiLCs molecularly and morphologically mimic EpiSCs (30). In agreement, Xist and X-linked gene silencing are ectopically induced only when $X^{\Delta Tsix}Y$ male and $X^{\Delta Tsix}X$ female EpiSCs differentiate (30). In fact, $X^{\Delta Tsix}Y$ and $X^{\Delta Tsix}X$ embryonic epiblasts, ESCs, and EpiSCs all display ectopic Xist induction and X-linked gene silencing as a function of differentiation, rather than developmental timing (30).

The X-chromosome dosage effect in the Tsix mutants may be intimately linked to the mechanism that senses, or "counts," the cellular X-chromosomal complement. The counting mechanism ensures that only if the X-chromosomal ploidy is sufficiently high does an X become targeted for inactivation. One prominent X-counting model invokes physical pairing of the two X chromosomes in females (62), via sequences within the *Xic*, including the *Tsix* locus, at the onset of X inactivation (63–65). As a consequence of this coupling, Xist is believed to be selectively upregulated from one of the two Xs (63–65), presumably through a transvection-like mechanism (62). However, deletions of all *Xic* elements thought to take part in X homolog pairing nevertheless result in Xist induction and inactivation of one of the two Xs in female cells (30, 33, 66–68).

Another mode of X-chromosomal dose sensing is the higher expression in *XX* cells of specific X-linked genes that lie within the *Xic*. The *Xic*-encoded *Ftx* and *Jpx*/*Enox* lncRNAs, both of which are expressed from the active and the inactive X chromosomes, are believed to facilitate X inactivation by activating Xist (19, 69, 70). Similarly, the *Rnf12* protein-coding gene, also encoded within the *Xic* but subject to X inactivation, is also posited to induce Xist through its higher expression in females before inactivation (67, 71, 72). However, a deletion of the *Xic* segment encompassing all three of these factors does not prevent Xist induction or gene silencing, since the mutant X chromosome

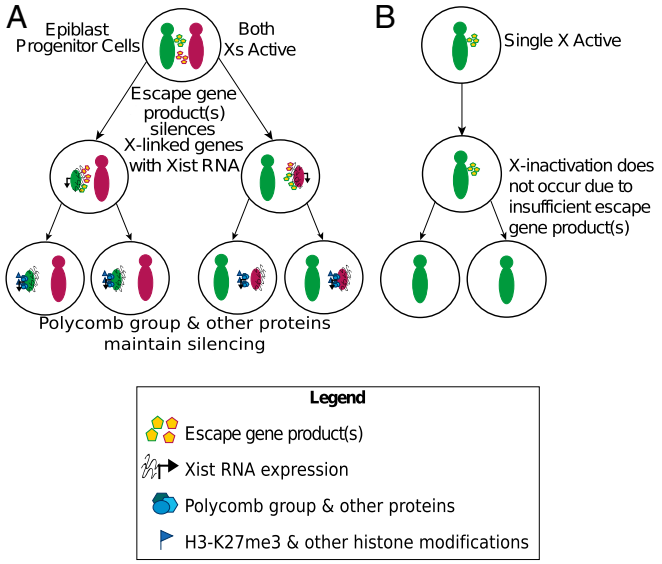

Fig. 6. A model of random X-inactivation initiation by X-inactivation escapee(s). *XX* female pluripotent epiblast progenitor cells (*A*) have two active X chromosomes and express the products of the escape gene(s) at equal levels from both. Upon differentiation, the 2× dose of the escape gene product(s) robustly induces Xist from the future inactive X. Once Xist is induced, the same or different escape gene product(s) cooperates with Xist to initiate silencing of genes on the inactive X chromosome. Polycomb group and other proteins then maintain silencing on the inactive X in part by depositing repressive histone marks. In *XY* males (*B*), the lower dose of the escape gene product(s) is insufficient to induce Xist and to silence X-linked genes.

is able to undergo Xist RNA coating and inactivation in differentiating ESCs (68).

These observations open the possibility of an alternate X-linked dosage-sensing mechanism. Most X-linked genes in females with an inactive X chromosome are expressed at levels equal to that in males (73–75). A subset of X-linked genes, however, escape X inactivation in female cells and are capable of being expressed from both X chromosomes despite inactivation of one of the two Xs (76, 77). Due to expression from both alleles, these X-inactivation escapees are expressed at higher levels in females compared with males (78). We therefore suggest that the relatively higher expression of one or more X-inactivation escapees in females ectopically activates Xist expression as well as induces X-linked gene silencing in $X^{\Delta Tsix}X$ cells. The lower dosage of such factors in males may explain the reduced frequency of Xist induction and X-linked gene silencing in $X^{\Delta Tsix}Y$ cells. Similarly, female $X^{\Delta Tsix}O$ cells lack a second X chromosome, and, like males, would have a lower dosage of X-inactivation escapees compared with $X^{\Delta Tsix}X$ females. The dose-dependent effect of the X-inactivation escapees implies that they function as diffusible/*trans*-acting factors.

The escapees in $X^{\Delta Tsix}X$ mutants are also expected to escape X inactivation in WT *XX* cells. In the Tsix mutants, we propose that Xist is induced in both males and females by the escapees due to the lower threshold conferred by Tsix absence (30). In WT cells, the same dose of the escapees activates Xist only in females and not in males due to an intact Tsix locus (Fig. 6). Thus, we postulate that one or more X-inactivation escapees normally induces Xist from the future inactive X in WT *XX* females.

Once Xist is induced, the same, or a different, escape gene product may silence X-chromosomal genes cooperatively with Xist, either by interacting with Xist RNA or through a parallel pathway. Recent reports of proteins bound to Xist found two X-encoded proteins, NONO and RBM3, as direct Xist RNA partners (14, 15). Neither gene, however, escapes random X inactivation (77, 78). The critical escapee proteins may therefore only indirectly or transiently interact with Xist, or may indirectly induce Xist and X-linked gene silencing. Alternatively, the catalog of Xist-binding proteins may be incomplete (14, 15). Consistent with the dose-dependent function of the escapee(s) in triggering X inactivation, ESCs with supernumerary X chromosomes display faster kinetics of Xist induction and X inactivation, commensurate with the number of extra X chromosomes (33). By inducing Xist and X-linked gene silencing in a dose-dependent manner, the escapee(s) thus also serve as X-chromosomal counting factor(s).

The increased dose of one or more X-chromosomal genes is believed to underlie DNA methylation differences between male and female ESCs. Bulk DNA in *XX* ESCs is hypomethylated relative to *XY* ESCs (79). The same X-linked factor(s) may contribute to sex-specific differences in Xist induction and X-linked gene silencing. However, *XX* female somatic cells with an inactive X chromosome do not display reduced DNA methylation levels compared with *XY* male cells (79), suggesting that the effect is not modulated by X-inactivation escapees. Nevertheless, early X-inactivated cells such as female EpiSCs may be hypomethylated compared with male EpiSCs, potentially implicating the same X-inactivation escapee(s) in regulating both DNA hypomethylation and X inactivation.

The *Xic* is an obvious X-chromosomal segment where the candidate escapee genes may reside. Classical mouse and human studies of X-chromosome truncations, translocations, and deletions, pinpointed the *Xic* as necessary for initiating random X inactivation (19, 32, 80–83). Expectedly, the Xist locus maps to the *Xic* (9). The *Xic*, however, may not be sufficient to recapitulate the various steps underlying random X inactivation, including the sensing of the X-chromosomal dose, as suggested by the inability of large single-copy YAC *Xic* transgenes to induce Xist (28, 29). A recent report delineating X-inactivation escapees in ESCs via allele-specific RNA-seq may yield candidate X-inactivation regulators (77). It is also plausible that the escapees indirectly control Xist induction and gene silencing by up-regulating the active allele of a gene(s) that is subject to X inactivation, inducing other escapees, or triggering the sex-specific expression of autosomal factors. We are currently defining the repertoire of X-inactivation escapees in EpiSCs, to investigate which escape genes function as dosage-sensitive factors that induce Xist and trigger X-linked gene silencing.

Materials and Methods

This study was performed in strict accordance with the recommendations in the *Guide for the Care and Use of Laboratory Animals* of the National Institutes of Health (84). All animals were handled according to protocols approved by the University Committee on Use and Care of Animals (UCUCA) at the University of Michigan (protocol #PRO00004007).

ESC and EpiSC derivation, RNA/DNA FISH, immunofluorescence (IF), RT-PCR, pyrosequencing, cell proliferation, viability assays, microscopy, and the mice used in this study have previously been described in ref. 30 and are detailed in *SI Appendix*.

ACKNOWLEDGMENTS. We thank members of the S.K. laboratory for discussions and critical review of the manuscript; Shigeki Iwase and Jacob Mueller for critically evaluating the manuscript; Angela Andersen of Pickersgill and Andersen, Life Science Editors (lifescienceeditors.com/), for editing services; and we acknowledge the services of the University of Michigan Sequencing Core Facility, supported in part by the University of Michigan Comprehensive Cancer Center. This work was funded by an NIH National Research Service Award 5-T32-GM07544 from the National Institute of General Medicine Sciences (to E.M.), a University of Michigan Reproductive Sciences Program training grant, NIH National Research Service Award 1F31HD080280-01 from the National Institute of Child Health and Human Development (to E.M.), a Rackham Predoctoral Fellowship from the University of Michigan (to E.M.), an NIH Director's New Innovator Award (DP2-OD-008646-01) (to S.K.), a March of Dimes Basil O'Connor Starter Scholar Research Award (5-FY12-119) (to S.K.), and the University of Michigan Endowment for Basic Sciences.

1. Lyon MF (1961) Gene action in the X-chromosome of the mouse (Mus musculus L.). *Nature* 190:372–373.
2. Morey C, Avner P (2011) The demoiselle of X-inactivation: 50 years old and as trendy and mesmerising as ever. *PLoS Genet* 7(7):e1002212.
3. Lee JT, Bartolomei MS (2013) X-inactivation, imprinting, and long noncoding RNAs in health and disease. *Cell* 152(6):1308–1323.
4. Barakat TS, Jonkers I, Monkhorst K, Gribnau J (2010) X-changing information on X inactivation. *Exp Cell Res* 316(5):679–687.
5. Chow J, Heard E (2009) X inactivation and the complexities of silencing a sex chromosome. *Curr Opin Cell Biol* 21(3):359–366.
6. Penny GD, Kay GF, Sheardown SA, Rastan S, Brockdorff N (1996) Requirement for Xist in X chromosome inactivation. *Nature* 379(6561):131–137.
7. Marahrens Y, Loring J, Jaenisch R (1998) Role of the Xist gene in X chromosome choosing. *Cell* 92(5):657–664.
8. Marahrens Y, Panning B, Dausman J, Strauss W, Jaenisch R (1997) Xist-deficient mice are defective in dosage compensation but not spermatogenesis. *Genes Dev* 11(2): 156–166.
9. Brown CJ, et al. (1991) A gene from the region of the human X inactivation centre is expressed exclusively from the inactive X chromosome. *Nature* 349(6304):38–44.
10. Brown CJ, et al. (1992) The human XIST gene: Analysis of a 17 kb inactive X-specific RNA that contains conserved repeats and is highly localized within the nucleus. *Cell* 71(3):527–542.
11. Clemson CM, McNeil JA, Willard HF, Lawrence JB (1996) XIST RNA paints the inactive X chromosome at interphase: Evidence for a novel RNA involved in nuclear/chromosome structure. *J Cell Biol* 132(3):259–275.
12. Panning B, Jaenisch R (1996) DNA hypomethylation can activate Xist expression and silence X-linked genes. *Genes Dev* 10(16):1991–2002.
13. Lee JT (2011) Gracefully ageing at 50, X-chromosome inactivation becomes a paradigm for RNA and chromatin control. *Nat Rev Mol Cell Biol* 12(12):815–826.
14. Chu C, et al. (2015) Systematic discovery of Xist RNA binding proteins. *Cell* 161(2):404–416.
15. McHugh CA, et al. (2015) The Xist lncRNA interacts directly with SHARP to silence transcription through HDAC3. *Nature* 521(7551):232–236.
16. Kalantry S, Purushothaman S, Bowen RB, Starmer J, Magnuson T (2009) Evidence of Xist RNA-independent initiation of mouse imprinted X-chromosome inactivation. *Nature* 460(7255):647–651.
17. Takagi N, Sasaki M (1975) Preferential inactivation of the paternally derived X chromosome in the extraembryonic membranes of the mouse. *Nature* 256(5519):640–642.
18. Gribnau J, Luikenhuis S, Hochedlinger K, Monkhorst K, Jaenisch R (2005) X chromosome choice occurs independently of asynchronous replication timing. *J Cell Biol* 168(3):365–373.
19. Maclary E, Hinten M, Harris C, Kalantry S (2013) Long nonoding RNAs in the X-inactivation center. *Chromosome Res* 21(6–7):601–614.
20. Jiang J, et al. (2013) Translating dosage compensation to trisomy 21. *Nature* 500(7462): 296–300.

21. Bala Tannan N, et al. (2014) DNA methylation profiling in X;autosome translocations supports a role for L1 repeats in the spread of X chromosome inactivation. *Hum Mol Genet* 23(5):1224–1236.
22. Cotton AM, et al. (2014) Spread of X-chromosome inactivation into autosomal sequences: Role for DNA elements, chromatin features and chromosomal domains. *Hum Mol Genet* 23(5):1211–1223.
23. Herzing LB, Romer JT, Horn JM, Ashworth A (1997) Xist has properties of the X-chromosome inactivation centre. *Nature* 386(6622):272–275.
24. Lee JT, Jaenisch R (1997) Long-range cis effects of ectopic X-inactivation centres on a mouse autosome. *Nature* 386(6622):275–279.
25. Tang YA, et al. (2010) Efficiency of Xist-mediated silencing on autosomes is linked to chromosomal domain organisation. *Epigenetics Chromatin* 3(1):10.
26. Wutz A, Jaenisch R (2000) A shift from reversible to irreversible X inactivation is triggered during ES cell differentiation. *Mol Cell* 5(4):695–705.
27. Wutz A, Rasmussen TP, Jaenisch R (2002) Chromosomal silencing and localization are mediated by different domains of Xist RNA. *Nat Genet* 30(2):167–174.
28. Heard E, Mongelard F, Arnaud D, Avner P (1999) Xist yeast artificial chromosome transgenes function as X-inactivation centers only in multicopy arrays and not as single copies. *Mol Cell Biol* 19(4):3156–3166.
29. Heard E, et al. (1996) Transgenic mice carrying an Xist-containing YAC. *Hum Mol Genet* 5(4):441–450.
30. Gayen S, Maclary E, Buttigieg E, Hinten M, Kalantry S (2015) A primary role for the Tsix lncRNA in maintaining random X-chromosome inactivation. *Cell Reports* 11(8): 1251–1265.
31. Sado T, Wang Z, Sasaki H, Li E (2001) Regulation of imprinted X-chromosome inactivation in mice by Tsix. *Development* 128(8):1275–1286.
32. Rastan S, Robertson EJ (1985) X-chromosome deletions in embryo-derived (EK) cell lines associated with lack of X-chromosome inactivation. *J Embryol Exp Morphol* 90: 379–388.
33. Monkhorst K, Jonkers I, Rentmeester E, Grosveld F, Gribnau J (2008) X inactivation counting and choice is a stochastic process: Evidence for involvement of an X-linked activator. *Cell* 132(3):410–421.
34. Namekawa SH, Payer B, Huynh KD, Jaenisch R, Lee JT (2010) Two-step imprinted X inactivation: Repeat versus genic silencing in the mouse. *Mol Cell Biol* 30(13): 3187–3205.
35. Patrat C, et al. (2009) Dynamic changes in paternal X-chromosome activity during imprinted X-chromosome inactivation in mice. *Proc Natl Acad Sci USA* 106(13): 5198–5203.
36. Margueron R, Reinberg D (2011) The Polycomb complex PRC2 and its mark in life. *Nature* 469(7330):343–349.
37. Plath K, et al. (2003) Role of histone H3 lysine 27 methylation in X inactivation. *Science* 300(5616):131–135.
38. Silva J, et al. (2003) Establishment of histone h3 methylation on the inactive X chromosome requires transient recruitment of Eed-Enx1 polycomb group complexes. *Dev Cell* 4(4):481–495.
39. Tesar PJ, et al. (2007) New cell lines from mouse epiblast share defining features with human embryonic stem cells. *Nature* 448(7150):196–199.
40. Brons IG, et al. (2007) Derivation of pluripotent epiblast stem cells from mammalian embryos. *Nature* 448(7150):191–195.
41. Pasque V, Gillich A, Garrett N, Gurdon JB (2011) Histone variant macroH2A confers resistance to nuclear reprogramming. *EMBO J* 30(12):2373–2387.
42. Bao S, et al. (2009) Epigenetic reversion of post-implantation epiblast to pluripotent embryonic stem cells. *Nature* 461(7268):1292–1295.
43. Chadwick LH, Pertz LM, Broman KW, Bartolomei MS, Willard HF (2006) Genetic control of X chromosome inactivation in mice: Definition of the Xce candidate interval. *Genetics* 173(4):2103–2110.
44. Johnston PG, Cattanach BM (1981) Controlling elements in the mouse. IV. Evidence of non-random X-inactivation. *Genet Res* 37(2):151–160.
45. Ohhata T, Hoki Y, Sasaki H, Sado T (2008) Crucial role of antisense transcription across the Xist promoter in Tsix-mediated Xist chromatin modification. *Development* 135(2): 227–235.
46. Kalantry S, Magnuson T (2006) The Polycomb group protein EED is dispensable for the initiation of random X-chromosome inactivation. *PLoS Genet* 2(5):e66.
47. Grumbach MM, Morishima A, Taylor JH (1963) Human sex chromosome abnormalities in relation to DNA replication and heterochromatinization. *Proc Natl Acad Sci USA* 49(5):581–589.
48. Lyon MF (1962) Sex chromatin and gene action in the mammalian X-chromosome. *Am J Hum Genet* 14:135–148.
49. Speirs S, Cross JM, Kaufman MH (1990) The pattern of X-chromosome inactivation in the embryonic and extra-embryonic tissues of post-implantation digynic triploid LT/Sv strain mouse embryos. *Genet Res* 56(2-3):107–114.
50. Webb S, de Vries TJ, Kaufman MH (1992) The differential staining pattern of the X chromosome in the embryonic and extraembryonic tissues of postimplantation homozygous tetraploid mouse embryos. *Genet Res* 59(3):205–214.
51. Monkhorst K, et al. (2009) The probability to initiate X chromosome inactivation is determined by the X to autosomal ratio and X chromosome specific allelic properties. *PLoS One* 4(5):e5616.
52. Cohen DE, et al. (2007) The DXPas34 repeat regulates random and imprinted X inactivation. *Dev Cell* 12(1):57–71.
53. Navarro P, et al. (2010) Molecular coupling of Tsix regulation and pluripotency. *Nature* 468(7322):457–460.
54. Stavropoulos N, Rowntree RK, Lee JT (2005) Identification of developmentally specific enhancers for Tsix in the regulation of X chromosome inactivation. *Mol Cell Biol* 25(7): 2757–2769.
55. Vigneau S, Augui S, Navarro P, Avner P, Clerc P (2006) An essential role for the DXPas34 tandem repeat and Tsix transcription in the counting process of X chromosome inactivation. *Proc Natl Acad Sci USA* 103(19):7390–7395.
56. Maclary E, et al. (2014) Differentiation-dependent requirement of Tsix long noncoding RNA in imprinted X-chromosome inactivation. *Nat Commun* 5:4209.
57. Nora EP, et al. (2012) Spatial partitioning of the regulatory landscape of the X-inactivation centre. *Nature* 485(7398):381–385.
58. Tsai CL, Rowntree RK, Cohen DE, Lee JT (2008) Higher order chromatin structure at the X-inactivation center via looping DNA. *Dev Biol* 319(2):416–425.
59. Burgoyne PS, et al. (1995) The genetic basis of XX-XY differences present before gonadal sex differentiation in the mouse. *Philos Trans R Soc Lond B Biol Sci* 350(1333): 253–260, discussion 260–251.
60. Nagy A, Gertsenstein M, Vintersten K, Behringer RR (2003) *Manipulating the Mouse Embryo: A Laboratory Manual* (Cold Spring Harbor Lab Press, Cold Spring Harbor, NY), p 71.
61. Snow MHL (1977) Gastrulation in the mouse: Growth and regionalization of the epiblast. *J Embryol Exp Morphol* 42:293–303.
62. Marahrens Y (1999) X-inactivation by chromosomal pairing events. *Genes Dev* 13(20): 2624–2632.
63. Augui S, et al. (2007) Sensing X chromosome pairs before X inactivation via a novel X-pairing region of the Xic. *Science* 318(5856):1632–1636.
64. Bacher CP, et al. (2006) Transient colocalization of X-inactivation centres accompanies the initiation of X inactivation. *Nat Cell Biol* 8(3):293–299.
65. Xu N, Tsai CL, Lee JT (2006) Transient homologous chromosome pairing marks the onset of X inactivation. *Science* 311(5764):1149–1152.
66. Sun S, Fukue Y, Nolen L, Sadreyev R, Lee JT (2010) Characterization of Xpr (Xpct) reveals instability but no effects on X-chromosome pairing or Xist expression. *Transcription* 1(1):46–56.
67. Jonkers I, et al. (2009) RNF12 is an X-encoded dose-dependent activator of X chromosome inactivation. *Cell* 139(5):999–1011.
68. Barakat TS, et al. (2014) The trans-activator RNF12 and cis-acting elements effectuate X chromosome inactivation independent of X-pairing. *Mol Cell* 53(6):965–978.
69. Chureau C, et al. (2011) Ftx is a non-coding RNA which affects Xist expression and chromatin structure within the X-inactivation center region. *Hum Mol Genet* 20(4): 705–718.
70. Tian D, Sun S, Lee JT (2010) The long noncoding RNA, Jpx, is a molecular switch for X chromosome inactivation. *Cell* 143(3):390–403.
71. Barakat TS, et al. (2011) RNF12 activates Xist and is essential for X chromosome inactivation. *PLoS Genet* 7(1):e1002001.
72. Gontan C, et al. (2012) RNF12 initiates X-chromosome inactivation by targeting REX1 for degradation. *Nature* 485(7398):386–390.
73. Deng X, Disteche CM (2010) Genomic responses to abnormal gene dosage: The X chromosome improved on a common strategy. *PLoS Biol* 8(2):e1000318.
74. Disteche CM (2012) Dosage compensation of the sex chromosomes. *Annu Rev Genet* 46:537–560.
75. Deng X, et al. (2011) Evidence for compensatory upregulation of expressed X-linked genes in mammals, Caenorhabditis elegans and Drosophila melanogaster. *Nat Genet* 43(12):1179–1185.
76. Berletch JB, Yang F, Disteche CM (2010) Escape from X inactivation in mice and humans. *Genome Biol* 11(6):213.
77. Marks H, et al. (2015) Dynamics of gene silencing during X inactivation using allele-specific RNA-seq. *Genome Biol* 16(1):149.
78. Berletch JB, et al. (2015) Escape from X inactivation varies in mouse tissues. *PLoS Genet* 11(3):e1005079.
79. Zvetkova I, et al. (2005) Global hypomethylation of the genome in XX embryonic stem cells. *Nat Genet* 37(11):1274–1279.
80. Augui S, Nora EP, Heard E (2011) Regulation of X-chromosome inactivation by the X-inactivation centre. *Nat Rev Genet* 12(6):429–442.
81. Brown CJ, et al. (1991) Localization of the X inactivation centre on the human X chromosome in Xq13. *Nature* 349(6304):82–84.
82. Takagi N (1980) Primary and secondary nonrandom X chromosome inactivation in early female mouse embryos carrying Searle's translocation T(X; 16)16H. *Chromosoma* 81(3):439–459.
83. Rastan S (1983) Non-random X-chromosome inactivation in mouse X-autosome translocation embryos—location of the inactivation centre. *J Embryol Exp Morphol* 78:1–22.
84. Committee on Care and Use of Laboratory Animals (1996) *Guide for the Care and Use of Laboratory Animals* (Natl Inst Health, Bethesda), DHHS Publ No (NIH) 85-23.